Rapid Communications

Large magnetoresistance by Pauli blockade in hydrogenated graphene

J. Guillemette,[1,2] N. Hemsworth,[3] A. Vlasov,[3] J. Kirman,[3] F. Mahvash,[3,4] P. L. Lévesque,[5] M. Siaj,[4] R. Martel,[5] G. Gervais,[1] S. Studenikin,[6] A. Sachrajda,[6] and T. Szkopek[3,*]

[1]*Department of Physics, McGill University, Montréal, Québec H3A 2A7, Canada*
[2]*Department of Physics, John Abbott College, Montréal, Québec H9X 3L9, Canada*
[3]*Department of Electrical and Computer Engineering, McGill University, Montréal, Québec H3A 2A7, Canada*
[4]*Department of Chemistry, Université du Québec à Montréal, Montréal, Québec H3C 3P8, Canada*
[5]*Department of Chemistry, Université de Montréal, Montréal, Québec H3C 3J7, Canada*
[6]*National Research Council Canada, 1200 Montreal Road, Ottawa, Ontario K1A 0R6, Canada*

We report the observation of a giant positive magnetoresistance in millimeter-scale hydrogenated graphene with the magnetic field oriented in the plane of the graphene sheet. A positive magnetoresistance in excess of 200% at a temperature of 300 mK was observed in this configuration, reverting to negative magnetoresistance with the magnetic field oriented normal to the graphene plane. We attribute the observed positive in-plane magnetoresistance to a Pauli blockade of hopping conduction induced by spin polarization. Our Rapid Communication shows that spin polarization in concert with electron-electron interaction can play a dominant role in magnetotransport within an atomic monolayer.

Giant magnetoresistance (GMR) is a manifestation of spin-dependent charge transport that encompasses a wide range of phenomena [1,2]. The strength of the GMR effect has led to its application in the sensing of magnetic fields, most importantly in high-density magnetic information storage. Here, we report the experimental discovery of a positive in-plane magnetoresistance (MR) reaching 235% in hydrogenated graphene, which we term large magnetoresistance (LMR). Similar hydrogenated graphene samples have shown a strong *negative* MR with the magnetic field applied normal to the sample surface, corresponding to a transition from an insulating state to a quantum Hall state [3,4]. The MR of a variety of functionalized graphene systems with the magnetic field applied normal to the graphene surface has been explored [5–7]. In contrast, we have observed a strong *positive* magnetoresistance with the magnetic field applied in plane. Considering the hopping conduction mechanism of hydrogenated graphene, it is the combination of spin polarization and electron-electron interaction that leads to positive LMR by a Pauli blockade of electron hopping as first described theoretically in the seminal work of Kamimura *et al.* [8].

Notably, the *quasi*-two-dimensional (2D) nature of a 2D electron system (2DES) can itself lead to a strong positive MR with the magnetic field applied in plane due to the finite layer thickness of the electron system. Nonperturbative magneto-orbital coupling arises when the magnetic length $\ell_B = \sqrt{h/eB_\parallel}$ approaches and becomes shorter than the rms thickness $\sqrt{\langle z^2 \rangle}$ of the 2DES [9]. Experimentally, positive in-plane MR has been observed in high-mobility Si field effect transistors [10–12], high-mobility GaAs/AlGaAs heterostructures and quantum wells [13–15], and Mn^{+2}-doped II-VI

quantum wells [16]. Singlet and triplet correlations in a high-mobility low-density 2DES have also been predicted to contribute to in-plane MR [17,18]. In-plane MR has been used as an experimental probe to gain insight into electron-electron interactions in the vicinity of the metal-insulator transition [19].

In the case of a graphene monolayer, the 2DES is confined to an atomic length scale of ~ 0.3 nm, which is orders of magnitude thinner than a typical 2DES hosted in a semiconductor heterostructure, leading to suppression of magneto-orbital effects. The resistivity of a pristine graphene monolayer encapsulated in boron nitride was measured with an in-plane magnetic field of up to $B_\parallel = 30$ T, corresponding to a magnetic length as short as $\ell_B \sim 4.7$ nm; in-plane MR was observed to be absent to within experimental error [20]. A weak in-plane MR of $\sim 3\%$ was observed in a graphene monolayer on a SiO_2 substrate as a result of magneto-orbital coupling through graphene ripples [21]. More recently, a positive in-plane MR of $\sim 5\%$ was observed in monolayer graphene on SiC and attributed to spin-dependent scattering at grain boundaries [22]. In-plane MR effects in graphene have thus far been observed to be comparatively small. We report here the observation of in-plane LMR in hydrogenated graphene where atomic thickness suppresses magneto-orbital MR and the primary effect of the in-plane magnetic field is to suppress hopping conduction via a Pauli blockade as first theoretically described by Kamimura *et al.* [8].

We conducted our experiments on millimeter-scale samples of monolayer graphene grown by chemical vapor deposition (CVD) [23] and transferred to degenerately doped silicon substrates with a 300-nm layer of oxide. Electrical contacts were fabricated either by direct mechanical application of In (sample HGT2) or by vacuum deposition of Ti/Au (3 nm/50 nm) through a shadow mask (samples HG18 and HG55). Hydrogenation was performed in an ultra-high-vacuum chamber with

*thomas.szkopek@mcgill.ca

an atomic hydrogen beam produced by thermal cracking of molecular hydrogen in a tungsten capillary heated by electron-beam bombardment [3]. Atomic hydrogen adsorbates create C-H bonds that disrupt the sp^2 lattice of graphene to create localized sp^3 distortions with a profound effect on graphene's electronic properties [24,25]. The neutral point defect density per carbon atom induced by hydrogenation in our samples is on the order of parts per thousand as inferred from Raman spectroscopy [3,4,26]. Direct experimental evidence for band-gap opening and the appearance of localized states in hydrogenated graphene was reported using angle-resolved photoemission spectroscopy (ARPES) and scanning tunneling spectroscopy [27–30].

We measured the electronic transport properties of hydrogenated graphene in the absence of a magnetic field, using standard lock-in detection techniques at a frequency of $f \sim 10$ Hz. The two-point resistance R_{2pt} versus gate voltage V_G at temperatures of $T = 5$–145 K are shown in Fig. 1(a) for the representative sample HG18. Strong insulating $\partial R_{2pt}/\partial T < 0$ is observed, indicative of the onset of electron localization by the introduction of neutral point defects into the graphene lattice via hydrogenation as previously reported [3,4,24,26]. The field effect corresponds to hole conduction $\partial R_{2pt}/\partial V_G > 0$ with a field effect mobility $\mu \propto \partial(1/R)/\partial V_G \to 0$ as $T \to 0$. The back-gate capacitance of $C_{ox} = 11.5$ nF/cm^2, leading to a modulation in the hole density of $\Delta p = C_{ox}V_G/e = 7.18 \times 10^{12}$/cm^2 over the swept gate voltage range of $V_G = 100$ V.

The MR of hydrogenated graphene sample HG18 was measured in a 32-T resistive magnet. The sample was mounted on a rotating sample mount to enable measurements with magnetic-field B applied in plane and out of plane relative to the graphene. The two-point resistance R_{2pt} versus in-plane and out-of-plane magnetic-field B is shown in Fig. 1(b) at a constant gate voltage of $V_G = -30$ V and temperature of $T = 320$ mK. Strong negative MR is observed with the magnetic field applied out of plane as previously reported [3]. In contrast, strong *positive* MR is observed with the magnetic field oriented in plane. The normalized MR is defined as $\Delta R_{2pt}(B)/R_{2pt}(0) = [R_{2pt}(B) - R_{2pt}(0)]/R_{2pt}(0)$ and reaches a value of 84% at $B = 32$ T. We ascribe the observed magnetoresistance to hydrogenation as opposed to the native disorder of CVD-grown graphene. A direct comparison of the normalized resistance $R_{2pt}(B)/R_{2pt}(0)$ versus in-plane magnetic-field B for two hydrogenated samples HG18 and HG55 and a pristine graphene sample G3 is shown in Fig. 1(c). There is no positive MR observed in pristine graphene, in agreement with Chiappini *et al.* [20]. We attribute the small negative MR observed with G3 to a residual out-of-plane magnetic-field component. For example, a misalignment between the in-plane field and the graphene plane of $0.6°$ at $B = 5$ T results in a 50-mT out-of-plane field that is sufficient to induce a negative MR of several percent due to weak localization [31].

The temperature dependence of the measured two-point resistance R_{2pt} versus in-plane magnetic-field $B_\parallel$ at a gate voltage of $V_G = -60$ V is shown in Fig. 1(d). A positive MR reaching $\Delta R_{2pt}(B)/R_{2pt}(0) = 235\%$ was observed at $T = 320$ mK. The positive LMR is in stark contrast with the comparatively weak positive MR of up to 5% reported in graphene samples under similar experimental conditions [20–22]. Both the re-
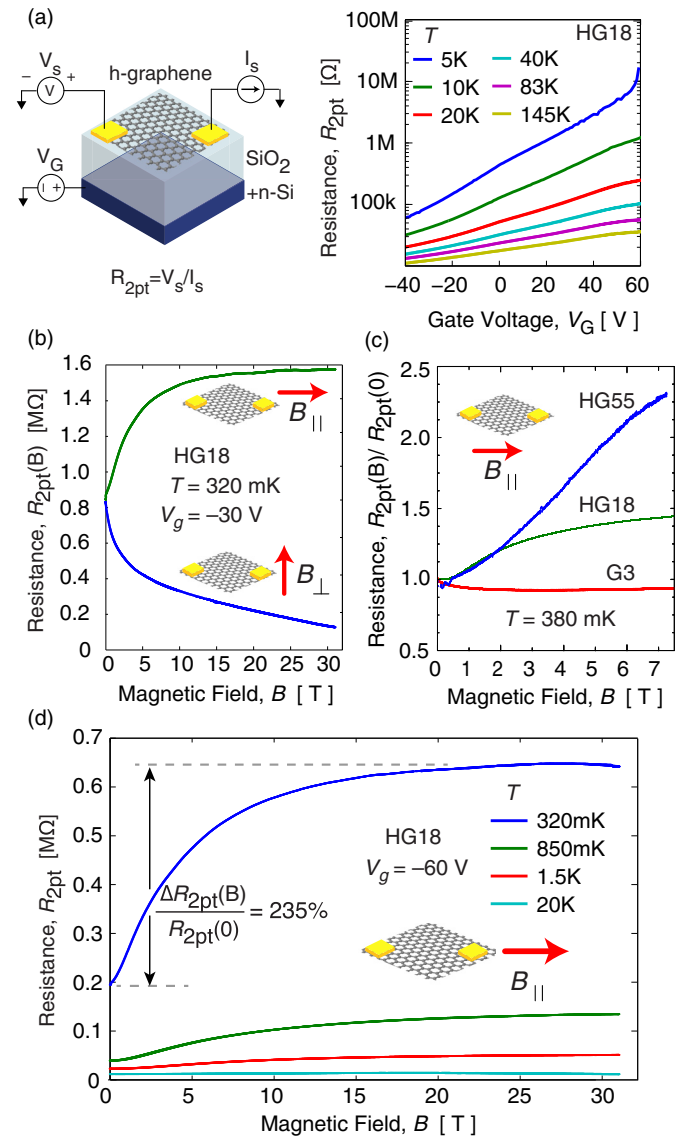

FIG. 1. The measured two-point resistance R_{2pt} of hydrogenated graphene sample HG18 at zero magnetic field versus back-gate voltage V_G is plotted in (a) at different temperatures T, showing strong insulating behavior and hole conduction. (b) The resistance $R_{2pt}(B)$ of sample HG18 is plotted versus magnetic-field B oriented in-plane $B_\parallel$ and out-of-plane $B_\perp$ to the graphene at $T = 320$ mK and $V_G = -30$ V. (c) Comparison of the normalized resistance $R_{2pt}(B)/R_{2pt}(0)$ versus in-plane magnetic-field B of hydrogenated samples HG18 and HG55 with the pristine graphene sample G3. (d) The temperature dependence of the resistance $R_{2pt}(B)$ of sample HG18 is plotted versus in-plane magnetic-field B at $V_G = -60$ V. A maximum magnetoresistance of $\Delta R_{2pt}(B)/R_{2pt}(0) = [R_{2pt}(B) - R_{2pt}(0)]/R_{2pt}(0) = 235\%$ is observed.

sistance and the MR are strongly suppressed as temperature increases with the MR dropping to $\Delta R_{2pt}(B)/R_{2pt}(0) = 125\%$ at $T = 1.5$ K and $\Delta R_{2pt}(B)/R_{2pt}(0) = 24\%$ at $T = 20$ K.

To further understand the nature of the magnetoresistance, the angular dependence was investigated with a sample mounted in a ^{3}He cryostat in a 5-T split coil superconducting magnet, allowing precise measurement (to $0.1°$) of increments in angle ϕ between the applied magnetic field and the graphene
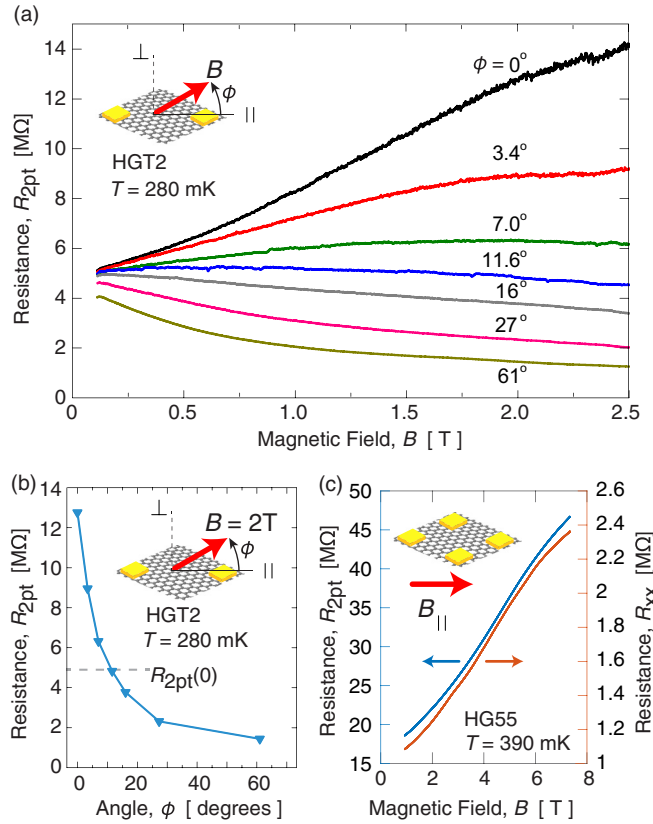
FIG. 2. (a) The measured two-point resistance R_{2pt} of hydrogenated graphene sample HGT2 versus magnetic-field B at a temperature of $T = 280$ mK with different field orientations indicated by angle ϕ. Positive MR with an in-plane field gives way to negative MR as the out-of-plane component increases. (b) The two-point resistance R_{2pt} versus angle ϕ at a fixed magnetic-field $B = 2.0$ T, showing the narrow peak in MR versus angle. The zero-field resistance $R_{2pt}(0)$ is indicated. (c) A comparison of the measured two-point resistance R_{2pt} and four-point resistance R_{xx} of hydrogenated graphene sample HG55 versus in-plane magnetic-field B at a temperature of $T = 390$ mK. Positive MR is observed in both two-point resistance R_{2pt} and four-point resistance R_{xx}.

plane. The two-point resistance R_{2pt} of hydrogenated graphene sample HGT2 versus applied magnetic-field B at various angles ϕ are illustrated in Fig. 2(a) at a temperature of $T = 280$ mK. As the applied field B is rotated out of the in-plane direction $\phi = 0°$, the positive MR is rapidly suppressed, and a transition to negative MR occurs at an angle of $7° < \phi < 12°$ for the magnetic-field range investigated as shown in Fig. 2(b). In other words, as the out-of-plane magnetic-field component $B_\perp = B \sin(\phi)$ increases, there is a transition from positive to negative MR.

Finally, we confirmed that the positive MR is a bulk effect in the hydrogenated graphene rather than a contact effect alone. Experiments were conducted in a ^{3}He cryostat with an 8-T superconducting solenoid and the sample mounted with the magnetic field in plane. A comparison of two-point resistance R_{2pt} and four-point resistance R_{xx} versus applied in-plane magnetic-field B is shown in Fig. 2(c) for a third sample HG55 with multiple contacts. Care was taken to use a high input impedance ($Z_{in} \sim 1$-TΩ) amplifier for four-point

measurement of the highly resistive sample. The two-point and four-point resistances both show a large positive MR, experimentally confirming that the bulk resistivity of hydrogenated graphene exhibits a positive LMR independent of the contact resistance.

We turn our attention to the underlying mechanism for positive MR in hydrogenated graphene with an in-plane field. It is instructive to compare several energy scales and length scales of the problem with a representative example provided by the observation of positive MR in excess of 100% at $B = 5$ T and $T = 320$ mK in sample HG18 as seen in Fig. 1(c). In these experimental conditions, the magnetic length $\ell_B = 11.6$ nm at $B = 5$ T is far greater than the effective 2DES thickness of $\sqrt{\langle z^2 \rangle} = 0.3$ nm in graphene. Thus, magneto-orbital effects are perturbative and small, in agreement with the absence of a measurable in-plane MR in pristine graphene [20]. In contrast, the polarization of electron spins is significant. The Zeeman splitting at $B = 5$ T is $g\mu_B B = 580$ μeV, which is significantly larger than the thermal energy $k_B T = 27.6$ μeV at $T = 320$ mK. In other words, $g\mu B/k_B T \gg 1$, and the spin degree of freedom of localized moments is strongly polarized at the B/T ratios for which in-plane LMR is observed. Lastly, the strongly insulating behavior $\partial R_{2pt}/\partial T < 0$ of hydrogenated graphene directly implies the onset of electron localization [3,4]. Electron transport proceeds by hopping conduction rather than band conduction.

Our observations are qualitatively consistent with the seminal theoretical work of Kamimura *et al.* [8], who was the first to show that the combination of spin polarization and electron-electron interaction can lead to strong positive MR in a localized electron system. Briefly, conduction in a localized system can proceed via one of four hopping processes involving unoccupied, singly occupied, and doubly occupied localized states as illustrated in Fig. 3(a). In a disordered system with on-site potential U, unoccupied, singly occupied, and doubly occupied localized states will all be present at energies in the vicinity of the chemical potential μ, and all states are thus available to participate in electron transport by hopping conduction. The exchange interaction is negligible for a pair of singly occupied sites (1,1) due to the negligible overlap of electron orbitals. This favors a triplet ground state in a magnetic-field B as shown in Fig. 3(b). In contrast, a doubly occupied site neighboring an empty site (2,0) has a non-negligible exchange energy J, favoring a singlet ground state as shown in Fig. 3(b). Spin polarization with an applied magnetic field thus suppresses electron hopping from a singly occupied site to a singly occupied site (1,1) $\rightarrow$ (0,2) by Pauli blockade as shown in Fig. 3(c). Detailed balance necessarily implies that the hopping process (2,0) $\rightarrow$ (1,1) is also suppressed. The net effect of spin polarization is an attenuation of hopping conduction through a subset of paths by the Pauli blockade mechanism, which leads to a suppression of conductance and hence a positive MR.

A detailed quantitative theory of positive MR was developed by Matveev *et al.* [32] for localized systems that exhibit Mott variable range hopping conduction and where cyclotron motion could be neglected. The model of Matveev *et al.* [32] assumes a *constant* density of localized states thus leading to a temperature-dependent conductivity $\sigma_{xx} = \sigma_0 \exp[-(T_0/T)^{1/d+1} F(x)]$, where $d = 2,3$ is the dimension
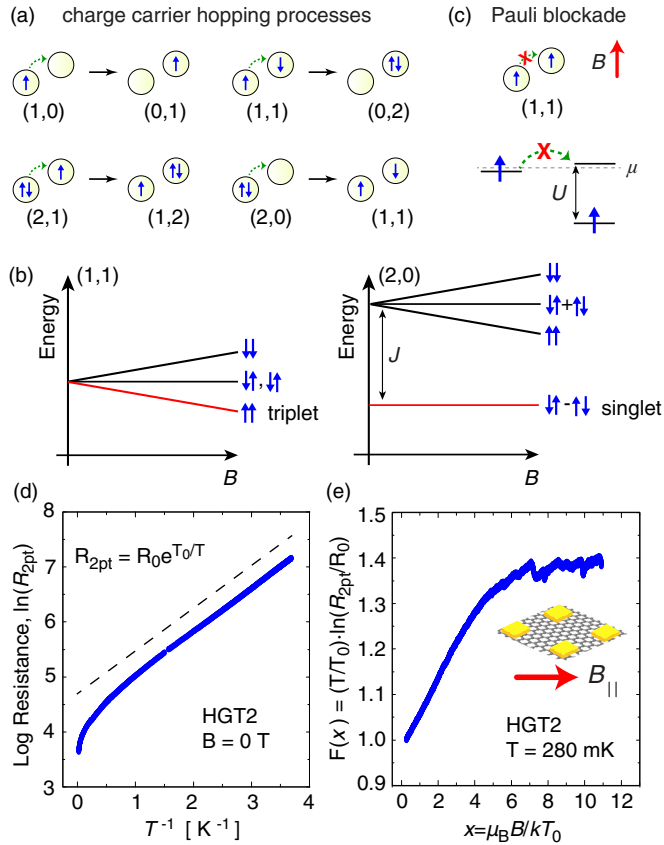
FIG. 3. (a) Schematic of four hopping processes among states with intrastate interaction: $(1,0) \to (0,1)$, a hop from a singly occupied state to an unoccupied state; $(1,1) \to (0,2)$, a hop from a singly occupied state to a singly occupied state; $(2,1) \to (1,2)$, a hop from a doubly occupied state to a singly occupied state; and $(2,0) \to (1,1)$, a hop from a doubly occupied state to an unoccupied state. (b) The $(1,1)$ ground state is a triplet, whereas exchange interaction J favors a singlet ground state for $(2,0)$. (c) As a consequence, spin polarization with a magnetic field suppresses the $(1,1) \to (0,2)$ hopping process by Pauli blockade. U is the on-site Coulomb interaction. (d) Measured resistance in natural logarithmic units versus reciprocal temperature of HGT2, showing an Arrhenius thermal activation for $T < 1$ K. (e) The exponent of magnetoresistance $F(x)$ versus the dimensionless parameter $x = \mu_B B / k T_0$, determined from the in-plane MR of HGT2 at $T = 280$ mK.

of the conductor, T_0 is the characteristic Mott temperature, and $F(x)$ is a universal function of a dimensionless magnetic-field parameter $x = \mu_B B / k_B T (T_0/T)^{1/d+1}$. Experimentally measured hydrogenated graphene resistivity does *not* follow a simple Mott variable range hopping law [3,4,26] (see the Supplemental Material [33]). The measured resistance of HGT2 in logarithmic scale versus reciprocal temperature $1/T$ at zero magnetic field is shown in Fig. 3(d) where agreement with $R = R_0 \exp(T_0/T)$ is observed for $T < 1$ K with $T_0 = 0.785$ K. We attribute the observed temperature dependence of resistance to an *energy-dependent* density of localized states, which leads to a modification of the Mott variable range hopping law exponent [34] that tends towards an Arrhenius-activated law $R = R_0 \exp(T_0/T)$ in the limit of a discontinuity in the density of localized states [35]. ARPES has indeed shown that the

density of localized states is not constant in hydrogenated graphene [27,28].

For comparative purposes, we analyze the resistance versus magnetic field using the analytical form derived in Matveev *et al.* [32] appropriate for an Arrhenius-activated law wherein $R = R_0 \exp[(T_0/T)F(x)]$ and $x = \mu_B B / k_B T_0$. The factor $F(x)$ for magnetoresistance can be extracted from measured magnetoresistance as $F(x) = (T/T_0) \ln(R/R_0)$ and is shown versus x for sample HGT2 in Fig. 3(e). Numerical computations of in-plane magnetoresistance and $F(x)$ for hydrogenated graphene are presently unavailable. Our experimentally determined $F(x)$ nonetheless adheres to two predictions in the analysis of Matveev *et al.* [32]: $F(x)$ has the linear form $F(x) \approx 1 + kx$ for $x \ll 1$, and $F(x) \to$ const for $x > x_{th}$, where k is a constant and x_{th} is a threshold for saturated magnetoresistance.

We now turn our attention to the tilted field regime. The strong suppression of positive MR with an out-of-plane magnetic-field component can be understood within this theoretical model. Spin polarization grows with the total field B, and thus the suppression of a subset of hopping conduction paths grows with the total applied field B. The positive MR effect evidently saturates as expected from the saturation of spin polarization [8,32] and as directly observed in our experiments [see Fig. 1(c)]. In contrast, the out-of-plane component $B_\perp = B \sin(\phi)$ induces in-plane cyclotron motion, suppressing backscattering to produce an overall enhancement of conduction. In the extreme limit, a transition from an insulating state to a quantum Hall state is observed at a high out-of-plane field [3]. Thus, experiments with an out-of-plane magnetic field conclusively demonstrate that the enhancement of conduction (negative MR) by in-plane cyclotron motion overwhelms the suppression of conduction (positive MR) by Pauli blockade. As a consequence, as the applied magnetic-field B increases, the positive MR peak versus angle ϕ (between B and the graphene plane) such as that shown in Fig. 2(b) is expected to sharpen around $\phi = 0°$. The narrow positive MR peak versus ϕ is thus a manifestation of the extreme anisotropy inherent to an atomically thin 2DES.

Our discovery of positive in-plane LMR in hydrogenated graphene is an experimental observation of the role of spin polarization on hopping conduction in a localized 2DES. The LMR appears at cryogenic temperatures alone where significant spin polarization can be developed by the applied in-plane field. Graphene and its hydrogenated derivative are a comparatively benign host for electron spins on account of the weak spin-orbit coupling present. Nonetheless, spin can play a dominant role in MR even in such a benign host due to the Pauli blockade mechanism. The in-plane MR of atomic monolayers and van der Waals heterostructures remains an underexplored area of research, whereas the development of atomically thin electronics exhibiting LMR is expected to be of interest for ultracompact magnetic sensing and information storage applications.

[1] A. Fert, Nobel Lecture: Origin, development, and future of spintronics, Rev. Mod. Phys. **80**, 1517 (2008).

[2] P. Grünberg, Nobel Lecture: From spin waves to giant magnetoresistance and beyond, Rev. Mod. Phys. **80**, 1531 (2008).

[3] J. Guillemette, S. S. Sabri, B. Wu, K. Bennaceur, P. E. Gaskell, M. Savard, P. L. Lévesque, F. Mahvash, A. Guermoune, M. Siaj, R. Martel, T. Szkopek, and G. Gervais, Quantum Hall Effect in Hydrogenated Graphene, Phys. Rev. Lett. **110**, 176801 (2013).

[4] K. Bennaceur, J. Guillemette, P. L. Lévesque, N. Cottenye, F. Mahvash, N. Hemsworth, A. Kumar, Y. Murata, S Heun, M.-O. Goerbig, C. Proust, M. Siaj, R. Martel, G. Gervais, and T. Szkopek, Measurement of topological Berry phase in highly disordered graphene, Phys. Rev. B **92**, 125410 (2015).

[5] X. Hong, S.-H. Cheng, C. Herding, and J. Zhu, Colossal negative magnetoresistance in dilute fluorinated graphene, Phys. Rev. B **83**, 085410 (2011).

[6] B. R. Matis, B. H. Houston, and J. W. Baldwin, Evidence for spin glass ordering near the weak to strong localization transition in hydrogenated graphene, ACS Nano **10**, 4857 (2016).

[7] S. Datta, Y. Cai, I. Yudhistira, Z. Zeng, Y.-W. Zhang, H. Zhang, S. Adam, J. Wu, and K. P. Loh, Tuning magnetoresistance in molybdenum disulphide and graphene using a molecular spin transition, Nat. Commun. **8**, 667 (2017).

[8] H. Kamimura, A. Kurobe, and T. Takemori, Magnetoresistance in Anderson-localized Systems, Physica B+C **117-118**, 652 (1983).

[9] S. Das Sarma and E. H. Hwang, Parallel Magnetic Field Induced Giant Magnetoresistance in Low Density Quasi-Two-Dimensional Layers, Phys. Rev. Lett. **84**, 5596 (2000).

[10] V. M. Pudalov, G. Brunthaler, A. Prinz, and G. Bauer, Instability of the two-dimensional metallic phase to a parallel magnetic field, Pis'ma Zh. Éksp. Teor. Fiz. **65**, 932 (1997).

[11] D. Simonian, S. V. Kravchenko, M. P. Sarachik, and V. M. Pudalov, Magnetic Field Suppression of the Conducting Phase in Two Dimensions, Phys. Rev. Lett. **79**, 2304 (1997).

[12] K. M. Mertes, D. Simonian, M. P. Sarachik, S. V. Kravchenko, and T. M. Klapwijk, Response to parallel magnetic field of a dilute two-dimensional electron system across the metal-insulator transition, Phys. Rev. B **60**, R5093 (1999).

[13] M. Y. Simmons, A. R. Hamilton, M. Pepper, E. H. Linfield, P. D. Rose, D. A. Ritchie, A. K. Savchenko, and T. G. Griffiths, Metal-Insulator Transition at B = 0 in a Dilute Two Dimensional GaAs-AlGaAs Hole Gas, Phys. Rev. Lett. **80**, 1292 (1998).

[14] J. Yoon, C. C. Li, D. Shahar, D. C. Tsui, and M. Shayegan, Parallel Magnetic Field Induced Transition in Transport in the Dilute Two-Dimensional Hole System in GaAs, Phys. Rev. Lett. **84**, 4421 (2000).

[15] X. Zhou, B. A. Piot, M. Bonin, L. W. Engel, S. Das Sarma, G. Gervais, L. N. Pfeiffer, and K. W. West, Colossal Magnetoresistance in an Ultraclean Weakly Interacting 2D Fermi Liquid, Phys. Rev. Lett. **104**, 216801 (2010).

[16] I. P. Smorchkova, N. Samarth, J. M. Kikkawa, and D. D. Awschalom, Giant magnetoresistance and quantum phase transitions in strongly localized magnetic two-dimensional electron gases, Phys. Rev. B **58**, 4238(R) (1998).

[17] G. Zala, B. N. Narozhny, and I. L. Aleiner, Interaction corrections at intermediate temperatures: Longitudinal conductivity and kinetic equation, Phys. Rev. B **64**, 214204 (2001).

[18] B. Spivak, S. V. Kravchenko, S. A. Kivelson, and X. P. A. Gao, Colloquium: Transport in strongly correlated two dimensional electron fluids, Rev. Mod. Phys. **82**, 1743 (1998).

[19] S. Anissimova, S. V. Kravchenko, A. Punnoose, A. M. Finkel'stein, and T. M. Klapwijk, Flow diagram of the metal-insulator transition in two dimensions, Nat. Phys. **3**, 707 (2007).

[20] F. Chiappini, S. Wiedmann, M. Titov, A. K. Geim, R. V. Gorbachev, E. Khestanova, A. Mishchenko, K. S. Novoselov, J. C. Maan, and U. Zeitler, Magnetotransport in single-layer graphene in a large parallel magnetic field, Phys. Rev. B **82**, 085302 (2010).

[21] M. B. Lundeberg and J. A. Folk, Rippled Graphene in an In-Plane Magnetic Field: Effects of a Random Vector Potential, Phys. Rev. Lett. **105**, 146804 (2010).

[22] H.-C. Wu, A. N. Chaika, M.-C. Hsu, T.-W. Huang, M. Abid, M. Abid, V. Y. Aristov, O. V. Molodtsova, S. V. Babenkov, Y. Niu, B. E. Murphy, S. A. Krasnikov, O. Lübben, H. Liu, B. S. Chun, Y. T. Janabi, S. N. Molotkov, I. V. Shvets, A. I. Lichtenstein, M. I. Katsnelson, and C.-R. Chang, Large positive in-plane magnetoresistance induced by localized states at nanodomain boundaries in graphene, Nat. Commun. **8**, 14453 (2017).

[23] A. Guermoune, T. Chari, F. Popescu, S. S. Sabri, J. Guillemette, H. S. Skulason, T. Szkopek, and M. Siaj, Chemical vapor deposition synthesis of graphene on copper with methanol, ethanol, and propanol precursors, Carbon **49**, 4204 (2011).

[24] D. C. Elias, R. R. Nair, T. M. G. Mohiuddin, S. V. Morozov, P. Blake, M. P. Halsall, A. C. Ferrari, D. W. Boukhvalov, M. I. Katsnelson, A. K. Geim, and K. S. Novoselov, Control of graphene's properties by reversible hydrogenation: Evidence for graphane, Science **323**, 610 (2009).

[25] J. Son, S. Lee, S. J. Kim, B. C. Park, H.-K. Lee, S. Kim, J. H. Kim, B. H. Hong, and J. Hong, Hydrogenated monolayer graphene with reversible and tunable wide band gap and its field-effect transistor, Nat. Commun. **7**, 13261 (2016).

[26] N. Hemsworth, F. Mahvash, P. L. Lévesque, M. Siaj, R. Martel, and T. Szkopek, Measurement of electronic heat dissipation in highly disordered graphene, Phys. Rev. B **92**, 241411(R) (2015).

[27] D. Haberer, D. V. Vyalikh, S. Taioli, B. Dora, M. Farjam, J. Fink, D. Marchenko, T. Pichler, K. Ziegler, S. Simonucci, M. S. Dresselhaus, M. Knupfer, B. Büchner, and A. Grüneis, Tunable band gap in hydrogenated quasi-free-standing graphene, Nano Lett. **10**, 3360 (2010).

[28] D. Haberer, L. Petaccia, M. Farjam, S. Taioli, S. A. Jafari, A. Nefedov, W. Zhang, L. Calliari, G. Scarduelli, B. Dora, D. V. Vyalikh, T. Pichler, C. Wöll, D. Alfè, S. Simonucci, M. S. Dresselhaus, M. Knupfer, B. Büchner, and A. Grüneis, Direct observation of a dispersionless impurity band in hydrogenated graphene, Phys. Rev. B **83**, 165433 (2011).

[29] M. Scheffler, D. Haberer, L. Petaccia, M. Farjam, R. Schlegel, D. Baumann, T. Hänke, A. Grüneis, M. Knupfer, C. Hess, and

B. Büchner, Probing local hydrogen impurities in quasi-free-standing graphene, ACS Nano **6**, 10590 (2012).

[30] S. Goler, C. Coletti, V. Tozzini, V. Piazza, T. Mashoff, F. Beltram, V. Pellegrini, and S. Heun, Influence of graphene curvature on hydrogen adsorption: Toward hydrogen storage devices, J. Phys. Chem. C **117**, 11506 (2013).

[31] A. M. R. Baker, J. A. Alexander-Webber, T. Altebaeumer, T. J. B. M. Janssen, A. Tzalenchuk, S. Lara-Avila, S. Kubatkin, R. Yakimova, C.-T. Lin, L.-J. Li, and R. J. Nicholas, Weak localization scattering lengths in epitaxial, and CVD graphene, Phys. Rev. B **86**, 235441 (2012).

[32] K. A. Matveev, L. I. Glazman, P. Clarke, D. Ephron, and M. R. Beasley, Theory of hopping magnetoresistance induced by Zeeman splitting, Phys. Rev. B **52**, 5289 (1995).

[33] See Supplemental Material at http://link.aps.org/supplemental/10.1103/PhysRevB.97.161402 for analysis of temperature-dependent resistance.

[34] A. G. Zabrodskii, The Coulomb gap: The view of an experimenter, Philos. Mag. B **81**, 1131 (2001).

[35] M. Pollak, A percolation treatment of dc hopping conduction, J. Non-Cryst. Solids **11**, 1 (1972).